Atmos. Chem. Phys. Discuss., 15, 20709–20741, 2015
www.atmos-chem-phys-discuss.net/15/20709/2015/
doi:10.5194/acpd-15-20709-2015


Atmospheric Chemistry and Physics Discussions
Open Access

This discussion paper is/has been under review for the journal Atmospheric Chemistry and Physics (ACP). Please refer to the corresponding final paper in ACP if available.

# Evaluation of VIIRS, GOCI, and MODIS Collection 6 AOD retrievals against ground sunphotometer measurements over East Asia

**Q. Xiao[1], H. Zhang[2], M. Choi[3], S. Li[1,4], S. Kondragunta[2], J. Kim[3], B. Holben[5], R. C. Levy[5], and Y. Liu[1]**

[1]Emory University, Rollins School of Public Health, Atlanta, GA, USA
[2]National Oceanic and Atmospheric Administration, Greenbelt, Maryland, USA
[3]Yonsei University, Seoul, South Korea
[4]State Key Laboratory of Remote Sensing Science, Beijing, China
[5]NASA Goddard Space Flight Center, Greenbelt, Maryland, USA

Received: 23 June 2015 – Accepted: 21 July 2015 – Published: 3 August 2015

Correspondence to: Y. Liu (yang.liu@emory.edu)

Published by Copernicus Publications on behalf of the European Geosciences Union.

## Abstract

Persistent high aerosol loadings together with extremely high population density have raised serious air quality and public health concerns in many urban centers in East Asia. However, ground based air quality monitoring is relatively limited in this area. Recently, satellite retrieved Aerosol Optical Depth (AOD) at high resolution has become a powerful tool to characterize aerosol patterns in space and time. Using ground AOD measurements from the Aerosol Robotic Network (AERONET) and the Distributed Regional Aerosol Gridded Observation Networks (DRAGON)-Asia Campaign, as well as from handheld sunphotometers, we evaluated emerging aerosol products from the Visible Infrared Imaging Radiometer Suite (VIIRS) aboard the Suomi National Polar-orbiting Partnership (S-NPP), the Geostationary Ocean Color Imager (GOCI) aboard the Communication, Ocean, and Meteorology Satellite (COMS), and Terra and Aqua Moderate Resolution Imaging Spectroradiometer (MODIS) (Collection 6) in East Asia in 2012 and 2013. In the case study in Beijing, when compared with AOD measured by handheld sunphotometers, 51 % of VIIRS Environmental Data Record (EDR) AOD, 33 % of VIIRS Intermediate Product (IP) AOD, 31 % of GOCI AOD, 26 % of Terra MODIS C6 3 km AOD, and 16 % of Aqua MODIS C6 3 km AOD fell within the reference expected error (EE) envelop ($\pm 0.05 \pm 0.15$ AOD). Comparing against AERONET measurements over the Japan–South Korea region, 64 % of EDR, 37 % of IP, 62 % of GOCI, 39 % of Terra MODIS and 56 % of Aqua MODIS C6 3 km AOD fell within the EE. In general, satellite aerosol products performed better in tracking the day-to-day variability than tracking the spatial variability at high resolutions. The VIIRS EDR and GOCI products provided the most accurate AOD retrievals, while VIIRS IP and MODIS C6 3 km products had positive biases.





ACPD
15, 20709–20741, 2015

Evaluation of VIIRS, GOCI, and MODIS Collection 6 AOD retrievals

Q. Xiao et al.

# 1 Introduction

The rapid economic growth and increasing fossil fuel usage have led to increasing air pollutant emission in East Asia. From 1980–2003, the emissions of black carbon, organic carbon, $SO_2$, and $NO_x$ increased by 28, 30, 119, and 176 %, respectively (Ohara et al., 2007). The continuous air quality degradation together with high population density have raised serious public health concerns in this region. Among commonly monitored air pollutants, particulate matter (PM), especially fine particulate matter ($PM_{2.5}$, airborne particles with an aerodynamic diameter less than or equal to 2.5 µm), is noted for its adverse health impacts, such as increased cardiovascular and respiratory morbidity and mortality (Pope III et al., 2009; Cao et al., 2012). The severe PM pollution in East Asia has attracted worldwide attention and ground PM monitoring networks have been developed in some East Asian countries, like China, Japan and South Korea. For instance, in South Korea, $PM_{10}$ together with other important air pollutants have been measured by a dense ground-based network, called "Air Korea", by the Ministry of Environment (https://www.airkorea.or.kr/eng/real/realTime). However, ground based monitoring networks have two main limitations: uneven distribution and limited coverage. For example, the majority of air quality monitoring stations in China are located in large cities and the monitoring network only covers about 360 out of the approximately 2860 municipalities. These two limitations of ground PM measurements result in insufficient information to conduct studies about PM sources, distribution, and consequent health impacts in East Asia, which can negatively impact policy making.

The extensive spatial coverage and growing time series of satellite retrievals allow researchers to better characterize aerosol patterns spatially and temporally. The most widely used satellite aerosol sensor, the Moderate Resolution Imaging Spectroradiometer (MODIS), has 36 spectral bands, acquiring data in wavelength from 0.41 to 15 µm and providing information about atmospheric aerosol properties (Remer et al., 2005). Two identical MODIS instruments are aboard the National Aeronautics and Space Administration (NASA) Terra and Aqua satellites, which fly over the study area at





ACPD
15, 20709–20741, 2015

around 10:30 and 13:30 LT, respectively. Several algorithms have been developed to retrieve aerosol optical depth (AOD) from MODIS data over land, such as the Dark-Target (Levy et al., 2013) algorithm and the Deep-Blue (Hsu et al., 2013) algorithm, providing AOD retrievals at 550 nm with global coverage. However, the widely used 10 km resolution MODIS aerosol products cannot depict urban-scale $PM_{2.5}$ heterogeneity (Cao et al., 2012). To resolve small-scale aerosol features, e.g. point $PM_{2.5}$ sources, and to assess the regional particle air pollution exposure, satellite aerosol products with higher resolutions and acceptable accuracy are urgently needed.

In response to the requirement of aerosol retrievals with higher spatial resolution, several emerging satellite aerosol products have become available recently. The Visible Infrared Imaging Radiometer Suite (VIIRS), is a multi-disciplinary scanning radiometer with 22 spectral bands covering from 0.412–12.05 µm and is designed as a new generation of operational satellite sensors that are able to provide aerosol products with similar quality to MODIS (Jackson et al., 2013). VIIRS is on board the NASA-NOAA Suomi National Polar-orbiting Partnership (S-NPP) launched in October 2011, and passes over the study area daily at approximately 1:30 p.m. LT. The VIIRS aerosol product reached validated maturity level in January 2013. The characteristics of the instrument and the aerosol retrieval algorithms are documented in detail elsewhere (Liu et al., 2014) and briefly described here. VIIRS provides two AOD products: the Intermediate Product (IP) and the Environmental Data Record (EDR). The VIIRS aerosol retrieval is performed at pixel level ($\sim 0.75$ km) spatial resolution globally as the IP that employs information from Navy Aerosol Analysis and Prediction System (NAAPS) and Global Aerosol Climatology Project (GACP) to fill in missing observations (Vermote et al., 2014). The IP is then aggregated to 6 km spatial resolution as the EDR, a level 2 aerosol product, through quality checking and excluding information from the NAAPS and GACP models. Both VIIRS IP and EDR are assigned quality flags of “high”, “degraded”, or “low” and valid AOD values range between 0.0 and 2.0. Previous global evaluation against AERONET AOD measurements over all land use types indicates that 71 % of EDR retrievals fell within the expected error (EE) envelope established by





ACPD
15, 20709–20741, 2015

MODIS level 2 aerosol products over land (±0.05±0.15 AOD), with a bias of −0.01 (Liu et al., 2014).

The Geostationary Ocean Color Imager (GOCI) is a geostationary Earth orbit sensor, providing hourly multi-spectral aerosol data eight times per day from 09:00 to 16:00 Korean LT. It covers a 2500 km × 2500 km sampling area, centered at [130° E, 36° N] in East Asia, at 500 m resolution with eight spectral channels at 412, 443, 490, 555, 660, 680, 745, and 865 nm, respectively (Lee et al., 2010). GOCI is aboard South Korea's Communication, Ocean, and Meteorology Satellite (COMS) that were launched in June 2010. The retrieval algorithm of its aerosol product, Yonsei aerosol retrieval algorithm, was originally based on the NASA MODIS algorithm and provides level 2 AOD retrievals at 6 km spatial resolution (Lee et al., 2010, 2012). The GOCI aerosol product allows AOD values range between −0.1 and 5.0. A previous study reported that during a two-month period (1 April to 31 May 2011), the GOCI AOD retrievals agreed well with the AERONET AOD measurements ($R^2 = 0.84$) over East Asia (Park et al., 2014).

To meet the need for finer resolution aerosol products, a 3 km aerosol product was introduced as part of the MODIS Collection 6 delivery. The 3 km aerosol product includes a quality flag ranging between 0 and 3 to indicate the quality of each retrieval and the valid AOD values range between −0.1 and 5.0. The retrieval algorithm of the 3 km product is documented in detail by Remer et al. (2013) and a global evaluation based on six months of Aqua data against ground sunphotometer AOD measurements indicates that 63 % of the retrievals fell into the EE with a bias of 0.03 over land (Remer et al., 2013). Munchak et al. (2013) reported that in the Baltimore–Washington, D.C. area, an urban/suburban region, 68 % of the 3 km retrievals from 20 June to 31 July 2011 fell into the EE with a bias of 0.013.

The release of these fine resolution satellite aerosol products has raised the question of whether these AOD retrievals can reflect the spatial pattern of aerosol loadings at their assigned resolutions. AERONET, a globally distributed federation of ground-based atmospheric aerosol measurements, provides reliable "ground truth" of AOD that are





ACPD
15, 20709–20741, 2015

widely used for the characterization of aerosol and validation of satellite retrievals (Eck et al., 1999; Holben et al., 1998). However, previous evaluation studies with AERONET data focused on the temporal accuracy, i.e. examined if the retrieved AOD can track the day-to-day variability of aerosol loadings. Evaluation of satellite aerosol products' ability to track small scale aerosol spatial variability is limited because the permanent AERONET stations can be tens or even hundreds of kilometers apart, leading to insufficient information required for a precise evaluation at high resolution. In response to the lack of ground AOD measurements at comparable spatial resolutions relative to satellite aerosol products, AERONET conducted several campaigns, which deployed additional temporary sunphotometers in selected regions and provided ground AOD measurements at a higher resolution. One of these campaigns, the Distributed Regional Aerosol Gridded Observation Network (DRAGON)-Asia Campaign in Japan and South Korea, lasted from 15 February to 31 May 2012 and provided a rare opportunity to validate these emerging satellite aerosol products (Petrenko et al., 2011; Sano et al., 2012). Another issue with previous evaluation studies is that few of them focused specifically on urban areas with higher pollution levels, greater disease burden and more complex aerosol patterns. Our work contributes to the validation effort of these emerging satellite products by employing ground measurements at finer resolution, extending the study period to one year, and conducting a mobile sampling experiment in the urban core of Beijing.

In this work, we quantitatively evaluate whether the latest VIIRS, GOCI and MODIS aerosol products can provide reliable AOD measurements and accurately characterize the spatial pattern of AOD over the urban areas in East Asia. Ground AOD measurements from AERONET, DRAGON-Asia, and handheld sunphotometers were collected over a period of one and a half years. The rest of the paper is organized such that Sect. 2, describes data sources and evaluation methods used in this study, Sect. 3 presents the performance of various satellite AOD products in representing intra city as well as regional variability of aerosol loadings. Finally, we summarize our findings and described future study directions in Sect. 4.





ACPD
15, 20709–20741, 2015

## 2 Data and methods

### 2.1 Study area

The study area is approximately 2500 km × 1100 km, centered at [128.5° E, 35.5° N] in East Asia, covering eastern China, South Korea and Japan (Fig. 1). This domain is within the overlapping region of all satellite datasets and ground measurements, and covers large urban centers, suburban areas, and rural areas. We also conducted a mobile sampling study in Metro Beijing along three major roads (Fig. 1). The study period is from January 2012 to June 2013.

### 2.2 Remote sensing data

The satellite aerosol products used in this study are from VIIRS, GOCI, Aqua MODIS and Terra MODIS sensors (Table 1). VIIRS data before May 2012 are not available because the sensor was in an early checkout phase and lacked a validated cloud mask (Liu et al., 2014). Thus, only EDR and IP pixels from May 2012 to June 2013 with high quality were processed. Similarly, GOCI aerosol retrievals from January 2012 to June 2013 were filtered by its assigned quality and only high quality (Quality Flag = 3) retrievals were included. The Aqua and Terra MODIS C6 3 km data from January 2012 to June 2013 were obtained from the Goddard Space Flight Center (http://ladsweb.nascom.nasa.gov/data). Only retrievals with high quality (Quality Flag = 3) were included in the analysis. The quality control criteria of these five satellite aerosol products are shown in Table 1.

### 2.3 Ground measurements

The characteristics of ground AOD measurement datasets are shown in Table 2. There were 18 permanent AERONET stations in the study area during the study period, supplemented by 24 temporary stations during the DRAGON-Asia Campaign. The DRAGON stations distributed nearly uniformly in two urban centers, Osaka in Japan

(7 stations) and Seoul in South Korea (11 stations), approximately 10 km apart. Other DRAGON stations were located across Japan and South Korea which can be tens to hundreds of kilometers apart. AERONET stations measure AOD at eight spectral bands between 340 and 1020 nm. To compare with satellite retrievals, AOD at 550 nm was calculated using a quadratic log-log fit from AERONET measurements at wavelengths 440 and 675 nm. Near-real time level 2.0 AERONET/DRAGON data in Japan–South Korea region and level 1.5 AERONET data in Beijing were downloaded from the Goddard Space Flight Center (http://aeronet.gsfc.nasa.gov/). The Level 1.5 AOD data are cloud-screened but not quality-assured (Smirnov et al., 2000); however, our preliminary results indicate that the level 1.5 daily average AOD values agreed well with the level 2.0 data, with a slope of 1.0 and zero intercept. Thus, we used the level 1.5 data in the case study in Beijing because level 2.0 data are not available for some AERONET stations.

To analyze the intra-city aerosol variability, we conducted ground measurements of AOD by a handheld sunphotometer (model 540 Microtops II, Solar Light Company, Inc.) at the Metro Beijing area in 2012 and 2013. Ground measurements were conducted on every cloud-free day at pre-selected sites that distributed roughly 6 km apart along the 3rd and the 5th Ring Roads and the Chang'an Avenue of Beijing. This sampling took place between 09:30 and 14:00 LT, and 5–10 repeated measurements were made at each site. To control the quality of the ground data, we used the median value of the repeated measurements as ground truth to eliminate the impact of extreme values and only included measurements with the ratio of standard deviation over median AOD less than 2.0. Our comparison of Microtops AOD measurements with nearby AERONET data yielded a slope of $\sim 0.95$ and a correlation coefficient of $\sim 0.8$ (Supplement, Text S1).

### 2.4 Data integration and analytical methods

All the data were reprojected to the JGD_2000_UTM_Zone_52N coordination system. For data integration, a 6 km grid and a 3 km grid covering the whole study domain were constructed, corresponding to the spatial resolution of each satellite product. Satellite aerosol data from different sensors were remapped to this 6 km grid (for VIIRS EDR and GOCI products) or 3 km grid (for VIIRS IP and MODIS C6 3 km products) with respect to their spatial resolution.

Two types of comparisons were conducted: the temporal comparison, which compared satellite AOD retrievals against ground measurements from AERONET stations during one year from July 2012 to June 2013; and the spatial comparison, which compared satellite AOD retrievals against high spatial resolution ground measurements from DRAGON stations or the handheld sunphotometer. The temporal comparisons and spatial comparisons differ in study periods (Table 2): the temporal comparison period was the longest overlap period covered by all five satellite products and the spatial comparison period allows the maximum sample size.

For the temporal comparison of VIIRS EDR data, we averaged valid AOD retrievals in each $3\times3$ grid cells sampling buffer (18 km $\times$ 18 km) centered at each ground AERONET station. The average AOD values were then compared with the mean AERONET AOD within a 1 h time window ($\pm$30 min around the satellite overpass time). We employed this smaller spatial averaging window than the widely used 27.5 km-radius-circle buffer suggested by the Multi-sensor Aerosol Products Sampling System (MAPSS) (Petrenko et al., 2011) in order to examine the performance of these finer resolution products at the scale of their expected application conditions. We used the typical 1 h time window because previous analysis indicates that changing the time window matters little to validation results (Remer et al., 2013) and the 1 h time window yields a larger database for the validation. For the spatial comparison of VIIRS EDR data, we used single 6 km pixels covering each ground measurement location, i.e. DRAGON station or handheld sunphotometer measurement location, and compared the AOD retrieval values with the mean AOD from the corresponding DRAGON station within the 1 h time window or the median AOD from the handheld sunphotometer at the corresponding location. The temporal and spatial comparisons of GOCI data followed the same protocol as described above. Although GOCI provides eight hourly AOD retrievals per day, we only





ACPD
15, 20709–20741, 2015

used the 13:00 LT retrievals in the comparison in order to make the validation results comparable among these satellite products.

For the temporal comparison of VIIRS IP data, we developed averaged valid AOD retrievals falling in the 3 km grid cell centered at each ground AERONET station. Since the IP pixel is at approximately 750 m spatial resolution, this sampling buffer averaged to a 4 × 4 pixel group. The average AOD values were compared against average AOD from the corresponding AERONET station within the 1 h time window. In the spatial comparison of VIIRS IP, we also used the 3 km sampling buffer due to the lack of ground measurements at finer resolutions. Thus, the VIIRS IP data is oversampled in the spatial comparison. For the temporal comparison of Aqua and Terra MODIS C6 3 km data, we employed the 3 km grid and averaged valid AOD retrievals in each 3 × 3 grid cells centered at each ground AERONET station to compare with the mean AOD within the 1 h time window. For the spatial comparison of MODIS C6 3 km data, we used the individual 3 km pixel AOD value falling on each ground measurement location to compare with average AOD from the corresponding DRAGON station within the 1 h time window or the median AOD from the handheld sunphotometer at the corresponding location.

In summary, for VIIRS EDR and GOCI products, the temporal and spatial comparison buffer was 18 km × 18 km and 6 km × 6 km, respectively. For the VIIRS IP product, the temporal and spatial comparison employed the same 3 km × 3 km buffer. For MODIS C6 3 km product, the temporal and spatial comparison buffer was 9 km × 9 km and 3 km × 3 km, respectively. The examples of buffers used in the temporal and spatial comparisons for each satellite products are shown in Supplement (Fig. S1). It is notable that both MODIS and VIIRS pixels were stretched toward the edge of the scan. For example, the 3 km × 3 km MODIS pixels become approximately 6 km × 12 km toward the edge. Thus, the remapping process and our construction of spatial comparison will slightly decrease the coverage for MODIS and VIIRS products and may potentially affect the spatial comparison results.





ACPD
15, 20709–20741, 2015

In epidemiological studies, in order to improve the coverage of satellite aerosol data to provide exposure estimates, spatial aggregation is widely used. In our analysis, we constructed quality flags for each matchup of satellite and ground AOD measurements to obtain better coverage without losing accuracy. For the temporal validation, matchups with at least 20 % coverage of both satellite data and ground measurements (Levy et al., 2013), e.g., having two or more satellite pixels within the sampling buffer and at least two AERONET/DRAGON measurements within the 1 h time window, were marked as "High Quality"; matchups with less than 20 % satellite pixels falling in the sampling buffer but one or more pixels located within the grid cell centered on the ground stations were marked as "Medium Quality"; while other matchups were marked as "Low Quality". In the spatial validation, because the best scenario matchup is supposed to have one or more satellite pixels within the one-grid cell sampling buffer and two or more AERONET/DRAGON measurements during the one hour time window, we only assigned two quality levels: "High Quality" for matches in the best scenario, and "Low Quality" for all others. Only matchups with high and medium quality were included in our validations and we also conducted a comparison, shown as Table S2, including all the matchups regardless of their quality to examine the influence of sampling bias. In addition, we conduct sensitivity analyses on VIIRS IP AOD retrievals including both high and degraded quality retrievals (Supplement, Table S1) and for the GOCI product at hourly scale (Supplement, Table S4) with respect to its eight hourly observations per day. In the hourly comparison, we constructed hourly average AERONET AOD as the ground measured true value and employed the same $3 \times 3$ grid cells temporal comparison sampling buffer.

## 2.5 Evaluation metrics

Several statistical metrics were used to describe the performance of satellite aerosol products in this study: coverage (%) describes the availability of site-day (or site-hour for GOCI data) satellite retrievals when the ground AERONET measurements were available in the temporal comparison; Pearson correlation coefficient describes the cor-





ACPD
15, 20709–20741, 2015

relation between satellite retrievals and ground AOD measurements; bias describes the average difference between satellite retrievals and ground AOD measurements; slope is the slope of the linear regression with satellite retrievals as the dependent variable and ground AOD measurements as the independent variable; and percent of retrievals falling within the expected error (EE) range. For the consistency of this metrics among different aerosol products, we employed the same EE, $\pm(0.05 + 0.15\text{AOD})$, that is established by MODIS C5 aerosol products over land in this study.

## 3 Results and discussion

### 3.1 Spatial variations of aerosol loadings

A previous study (Remer et al., 2005) indicated that the aerosol loading is homogeneous at horizontal scales within 200 km. However, that study is conducted over the ocean, which provides a homogeneous surface, leading to reduced aerosol spatial variability. The variability of aerosol loading at local scales in urban areas with complex land surface and meteorological conditions are expected to be greater. We assessed the intra city spatial variations of aerosol loadings over Beijing, Osaka, and Seoul with handheld sunphotometer and DRAGON-Asia AOD measurements in 2012. First, we calculated the great circle distance between each of two handheld sunphotometer measurement sites or DRAGON sites which are less than 20 km apart. Then we stratified the site to site distance by increments of 750 m and calculate the station to station correlation coefficient of daily average AOD within each distance stratum. The measurements from DRAGON sites in Osaka and Seoul and the measurements from handheld sunphotometers in Beijing were processed separately due to differences in instrumentation. Only handheld sunphotometer measurements in Beijing from 15 February to 31 May 2012 were included to ensure that the measurement period at these three locations is the same.





ACPD
15, 20709–20741, 2015

Figure 2a shows the correlation coefficient of daily AOD by binned distance and Fig. 2b shows the site specific average AOD with the regional average AOD subtracted in these three cities. Figure 2a indicates that the DRAGON AOD measurements were highly correlated within a 20 km spatial range with a correlation coefficient larger than 0.9. However, the result from handheld sunphotometer measurements in Beijing suggests that the spatial correlation coefficients declined slowly as the distance among two measurement locations increased up to 12 km. The correlation coefficient increased slightly when the distance among two measurement locations are beyond 12 km. This can be explained by the clustered distribution of ground measurement locations in Beijing: these long location-to-location distances only occur when the two locations are located along the Chang'an Avenue and vehicle exhaust is one of the major sources of aerosol in Beijing, thus these AOD measurements are highly correlated. The different aerosol spatial variability trends in Beijing and in the DRAGON domain can be attributed to the following reason: the DRAGON-Asia campaign provides real time observation but our ground measurement in Beijing provides one observation at each site per day, so that the average daily AOD from DRAGON may have smoothed away some of the spatial heterogeneity.

Even though the aerosol loadings are highly related spatially, the AOD value may differ among nearby stations (Fig. 2b). In Beijing, the difference in average AOD between two neighboring sites that are ~ 6 km apart can be as high as 0.4, about 49 % of the regional mean AOD value. The measurements from DRAGON stations show smaller difference in average AOD relative to that in Beijing, but the difference between two neighboring sites can still be greater than 0.1 in Seoul, 23 % of the regional mean AOD value. These results indicate that spatial contrast in aerosol loading exists at local scale and finer resolution satellite aerosol products are needed to better characterize individual and population exposure of particulate pollution.





ACPD
15, 20709–20741, 2015

### 3.2 The Beijing sampling experiment

The GOCI aerosol product provided the highest coverage in the temporal comparison over Beijing with 73 % available retrievals relative to AERONET measurements at 13:00, followed by the VIIRS IP (42 %), VIIRS EDR (41 %), MODIS Terra C6 3 km product (40 %), and MODIS Aqua C6 3 km product (38 %) (Supplement, Table S1). Table 3 shows the statistical metrics from the temporal and spatial comparisons over Beijing. In the temporal comparison, the GOCI product provided the most accurate AOD retrievals, which slightly overestimated AOD by 0.02 on average. Other aerosol products significantly overestimated AOD and the average bias in the temporal comparison for VIIRS EDR, VIIRS IP, Aqua and Terra MODIS C6 3 km products were 0.11, 0.25, 0.21, and 0.29, respectively. Though GOCI AOD retrievals agreed well with ground measurements in the temporal comparison, with 55 % of GOCI AOD retrievals at 13:00 falling within the EE, only 31 % of GOCI AOD retrievals fell within the EE in the spatial comparison. The comparison including all eight hourly GOCI observations represented reduced average hourly coverage (59 %), a smaller average bias (−0.006), and a larger proportion of retrievals fell within EE (59 %). Thus, the GOCI product resolved the temporal and spatial variability of aerosol loadings at its designed temporal and spatial resolutions, but it tracked the small-scale spatial variability less well than the temporal variability in Beijing.

VIIRS EDR product performed well in Beijing in both the temporal and spatial comparisons, with 52 and 51 % of retrievals fell within EE in the temporal and spatial comparison, respectively. Although VIIRS IP had a relatively large positive bias (0.25) in the temporal comparison, it provided acceptable coverage with 33 % retrievals falling within the EE in the spatial comparison, resolving valuable information of small-scale aerosol variability in urban areas. MODIS C6 3 km product had the largest high bias and lowest %EE in this spatial comparison, with 16 and 26 % of retrievals falling within the EE for Aqua and Terra MODIS, respectively. A previous validation study of the 3 km MODIS AOD data also reported similar retrieval errors in urban areas (Remer et al.,





ACPD
15, 20709–20741, 2015



Title Page
Abstract | Introduction
Conclusions | References
Tables | Figures
◀| |▶
◀ ▶
Back | Close
Full Screen / Esc
Printer-friendly Version
Interactive Discussion

2013). It is notable that the $R^2$ values of the MODIS C6 3 km products is the highest in the spatial comparisons (0.68 for Aqua and 0.85 for Terra) and the linear regression statistics indicates that the low percent of retrievals falling within EE is mainly due to a relatively constant positive offset: the intercepts for Aqua and Terra are 0.22 and 0.30, respectively. One possible explanation of the positive bias of MODIS and VIIRS products is that our study domain is highly urbanized with bright surfaces, therefore is challenging for the Dark Target algorithm.

### 3.3 The temporal evaluation of AOD over Japan–South Korea region

We first looked at the AOD retrievals distribution on one clear day, 7 May 2012, during the DROGAN period (Fig. 3). Figure 3 indicates that the sampling strategies and cloud masks differ in these five satellite aerosol products, resulting in different patterns of missing data. GOCI provided the best coverage with almost no missing data over this region. VIIRS products and MODIS products showed similar missing in the center of the map; while VIIRS products showed more missing in the lower right corner but MODIS products showed more missing in the upper right corner. VIIRS and MODIS pixels are stretched toward the edge of the scan. VIIRS and MODIS products tended to overestimate AOD values in the urban area (Seoul), but GOCI provided accurate AOD estimates in this region. Though these 3 km products showed similar spatial distribution patterns to the 6 km products, the 3 km products demonstrated greater heterogeneity, which is valuable to analyze local aerosol sources and estimate personal air pollution exposure.

Similar to the comparisons in Beijing, the GOCI aerosol products provided the highest coverage in the temporal comparison over Japan–South Korea region, with 74 % retrievals relative to AERONET measurements, followed by VIIRS EDR (63 %), VIIRS IP (50 %), Terra MODIS C6 3 km (26 %), and Aqua MODIS C6 3 km (24 %) (Supplement, Table S1). The distributions of the coincident satellite-AERONET AOD measurements with high or medium quality are shown in Fig. 4. The distribution of the Terra MODIS





ACPD
15, 20709–20741, 2015

Evaluation of VIIRS, GOCI, and MODIS Collection 6 AOD retrievals

Q. Xiao et al.

C6 product is not shown here because it passes the study region in the morning, leading to potential differences in AOD distribution relatives to other sensors that pass the study region in the afternoon. This histogram is plotted with relative frequency rather than the total number of retrievals because these aerosol products differ in sampling strategies, leading to different total number of matchups. VIIRS EDR, VIIRS IP, and GOCI products showed a similar mode of distribution to AERONET measurements, with the peak probability around 0.2. The distribution of Aqua MODIS C6 3 km AOD had the peak around 0.3, indicating that the Aqua MODIS C6 3 km product tended to overestimate AOD in general. A previous study also reported that the MODIS C6 3 km product had a decreased proportion of low AOD values and an increased proportion of high AOD values (Remer et al., 2013) relative to the 10 km product over land, leading to a higher global average AOD. The VIIRS IP product also tended to overestimate AOD, with higher percentage of retrievals occurring at high AOD values. The distribution of GOCI data provided the best fit with AERONET data, with a correlation coefficient of 0.95, followed by VIIRS EDR ($r = 0.93$), VIIRS IP ($r = 0.77$), and MODIS Aqua C6 3 km product ($r = 0.76$). The difference in the distributions of these satellite aerosol products can be partly explained by different retrieval assumptions including aerosol models, different surface reflectance and different global sampling strategies. Moreover, these satellite aerosol products differ in the valid AOD retrieval ranges, leading to differences in the distribution of extremely high and low AOD values.

The temporal comparisons over Japan–South Korea region showed more retrievals falling within the EE and smaller biases relative to comparisons in Beijing. Figure 5 is the frequency scatter plots showing the results of temporal comparisons over Japan–South Korea region and the corresponding box plots showing the difference between satellite AOD retrievals and ground observations. GOCI retrievals were highly correlated with the ground measurements with an $R^2$ of 0.80. The linear regression of GOCI retrievals and ground measurements fell close to the 1 : 1 line with a small average bias (0.04), and 62 % of GOCI retrievals at 13:00 fell in the EE (Table 4). Comparison including eight GOCI hourly retrievals showed a higher $R^2$ of 0.82 with a smaller aver-





ACPD
15, 20709–20741, 2015

age bias (0.01), and 66 % of retrievals fell in the EE (Table 4, GOCI all obs.). The box plot indicates that GOCI retrievals overestimated AOD at high AOD values (AOD > 0.6) (Fig. 5). Thus, the GOCI product tracked the daily variability of aerosol loadings well and it provided additional information to study short-term aerosol trends. Similarly, 64 % of VIIRS EDR retrievals fell into the EE with a slightly higher bias (0.05) and a slightly lower $R^2$ of 0.74 (Table 4). This positive bias is consistent with a previous global validation study, which reports a 0.01 bias of VIIRS EDR in East Asia (Liu et al., 2014). Though the VIIRS EDR product tended to overestimate AOD at low (AOD < 0.3) and high AOD values (AOD > 1.0), it agreed well with the AERONET measurements when AOD ranged between 0.3 and 1.0 (Fig. 5).

The VIIRS IP had linear regression slope close to 1 (1.03) against AERONET observations, but it had a consistent positive bias of 0.15 on average. Only 37 % of VIIRS IP retrievals fell within the EE. The scatter plot indicates that the IP retrievals varied substantially, especially when the AOD values were low. MODIS C6 3 km products had a high positive bias of 0.08 for Aqua and 0.16 for Terra. Consistent with what was reported by a previous global evaluation study, we observed that the MODIS C6 3 km products tended to overestimate AOD and the bias increased with AOD values (Remer et al., 2013). 56 % of the Aqua MODIS C6 3 km retrievals and 39 % of the Terra MODIS C6 3 km retrievals fell within the EE. In general, these finer resolution aerosol products included larger bias relative to the 6 km resolution products and researchers must be cautious when applying them.

Since the GOCI product provides eight hourly observations per day, to examine the temporal variability in the accuracy of GOCI aerosol retrievals, we compared the GOCI AOD retrievals with AERONET measurements stratified by hour (Supplement, Table S4). In general, the GOCI product provided high quality retrievals consistently throughout the day except that it tended to slightly overestimate AOD in the morning and underestimate AOD in the afternoon. Such temporal variability in accuracy was also reported by a previous evaluation study of the Geostationary Operational Environmental Satellite (GOES) aerosol product (Green et al., 2009). The daily variability in





ACPD
15, 20709–20741, 2015

the quality of GOCI retrievals may be due to changes in scattering angle, clouds and the associated Bidirectional Reflectance Distribution Function (BRDF) effects.

### 3.4 The spatial evaluation of AOD over Japan–South Korea region

The mean daily AOD from different sensors and AERONET stations during the one year period from July 2012 to June 2013 are shown in Fig. 6. These five aerosol products provided similar distribution of average AOD during the one year period, with the highest values occurred in northeastern China and the Yangtze River delta, and the lowest values occurred in southern China and Japan. Several high-AOD value spots appeared along the west coast of South Korea and surrounded the Seto Inland Sea, likely due to emissions from urban centers in these regions. These five maps differ in missing patterns due to their different masking approaches. The VIIRS algorithms did not retrieve AOD over inland lakes (e.g. the Taihu Lake); the GOCI product retrieved AOD over inland water; while MODIS products provided some AOD retrievals over inland lakes, with some missing data. The GOCI product did not provide high quality retrievals at some locations in central Japan due to snow coverage in this mountain region. To maintain a consistent evaluation data filtering strategy, the inland water AOD retrievals and ground observations were removed from the validation. The VIIRS EDR product showed lower AOD values in northeastern China and South Korea relative to AOD retrievals from other sensors. The VIIRS IP product also showed lower AOD values in northeastern China, but provided higher AOD retrievals in northern Japan. This can be explained by the system bias reported in a previous study that VIIRS retrievals tend to underestimate AOD when NDVI value is low and overestimate AOD over vegetated surface (Liu et al., 2014). The VIIRS IP product had higher AOD values relative to the EDR product, especially over the Korean Peninsula and northern Japan. This may be due to IP's ability to track small scale variability which were smoothed in the EDR retrievals, or may result from the positive bias of IP observed in the temporal comparison. Because VIIRS aerosol products restrict valid AOD values to between 0.0 and 2.0, they may underestimate AOD values when the aerosol loadings are extremely high, like in northeastern China, though lacking AERONET measurements in this region to test this hypothesis. Aqua and Terra MODIS C6 3 km aerosol products showed similar spatial distribution in AOD retrievals, with higher AOD values in urban areas, e.g. over the Yangtze River Delta and North China Plain in China. GOCI presented some high AOD values in local regions such as western South Korea, around the Seto Inland Sea, and over northeastern China. However, it showed lower AOD values over the Yangtze River Delta in China. This result is consistent with the temporal comparison results shown in Fig. 5 that the GOCI product slightly overestimated AOD at high AOD values (AOD > 0.6). Compared with the ground measurements, all these five aerosol products overestimated AOD in Japan, where the average AOD values were relatively low. VIIRS EDR tended to slightly underestimate AOD over the Seoul region. The lack of ground measurements, especially in northeast China, makes it impossible to quantitively evaluate the spatial distribution of these aerosol products in China.

Results of the spatial comparison over DRAGON-Asia region are shown in Table 4. Satellite aerosol products performed better in tracking the day-to-day variability relative to tracking their spatial patterns. In the spatial comparison, all the satellite aerosol products showed lower $R^2$ and larger offset with less retrievals falling into the EE. GOCI product provided the highest accuracy, with a small positive bias of 0.03 and 48 % of retrievals falling in the EE, followed by VIIRS EDR, with a positive offset of 0.16 and 41 % of retrievals falling in the EE. In contrast, VIIRS IP and MODIS C6 3 km had large positive offsets and less than 30 % of retrievals falling within the EE due to larger noise related with the finer resolution. The MODIS C6 3 km and VIIRS IP aerosol products introduced sporadic unrealistic high AOD retrievals over urban areas that are avoided more successfully by VIIRS EDR and GOCI products. Though these finer resolution aerosol products did not fully track the spatial trends of aerosol loading at their designed resolution, they provide additional information about aerosol spatial distribution and will benefit exposure assessments at local scales.

To examine possible sampling bias due to our data inclusion criteria, we performed temporal and spatial comparisons including all the matchups over Japan–South Korea region (Supplement, Table S2). There is no significant change in the evaluation metrics after including matchups with low quality. Thus, the validation results are robust and there is no evidence for sampling bias. We validated the VIIRS IP AOD retrievals with degraded quality over Japan–South Korea region and observed lower correlation coefficient, higher bias, and less retrievals falling within the EE in both the temporal and spatial comparisons (Supplement, Table S3). This result suggests to use only high quality VIIRS IP retrievals. We also validated the GOCI AOD retrievals with different quality over Japan–South Korea region. Including medium and low quality GOCI retrievals decreases the accuracy, but significantly increased the coverage (Supplement, Table S5). By including the retrievals with quality flag equals to both 3 and 2, the coverage increased from 27 to 38 % in the temporal comparison over the Japan–South Korea region, while the average bias increased by 0.01 and the percentage of retrievals falling within the EE decreased by 7 %. Thus, including retrievals with medium quality might be acceptable, depending on study objectives. Due to the relative small number of matched observations, analysis of the correlation between quality of satellite aerosol retrievals and satellite viewing angles were beyond the scope of this analysis. However, previous studies reported that towards the edge of the scan, VIIRS EDR tends to underestimate AOD over land (Liu et al., 2014).

## 4 Conclusions

In this work, the intra city variability of aerosol loadings were examined with ground measurements from the DRAGON-Asia campaign and our mobile sampling campaign in Beijing. Five emerging high resolution satellite aerosol products are evaluated by comparing them with ground measurements from AERONET, DRAGON, and hand-held sunphotometers over East Asia in 2012 and 2013. We observed variability in both correlation coefficient and average AOD values among ground AOD measurement sites in three urban centers in Asia. Evaluation results indicate that the 6 km resolution products, VIIRS EDR and GOCI, provided more accurate retrievals with higher coverage relative to the higher resolution products, VIIRS IP, Terra and Aqua MODIS C6 3 km products, in both temporal comparisons and spatial comparisons; satellite aerosol products resolved the day-to-day aerosol loading variability better than the spatial aerosol loading variability; satellite products performed less well in Beijing relative to in the Japan–South Korea region, indicating that retrieval in urban areas is challenging. The performance of these aerosol products in Beijing and at regional scale over Japan–South Korea region demonstrates that satellite aerosol products can track the small scale variability of aerosol loadings and high resolution satellite aerosol products provide valuable information for analyzing small scale air pollution, detecting point sources and estimating individual air pollution exposure. Future studies with additional ground measurements at small spatial and temporal scale will help us analyze air pollution patterns and further validate satellite products.

**The Supplement related to this article is available online at doi:10.5194/acpd-15-20709-2015-supplement.**

*Acknowledgement.* The work of Y. Liu and Q. Xiao was partially supported by the NASA Applied Sciences Program (grants NNX11AI53G and NNX14AG01G, PI: Y. Liu). We would like to acknowledge the AERONET team, I. Sano and the DRAGON-Japan team, the Yonsi team and their collaborators in S. Korea, and CARSNET and CAS teams in and around Beijing for providing data support in this study. The AERONET project is supported NASA EOS project office, and by Hal B. Maring, Radiation Sciences Program, NASA Headquarters.

## References


Cao, J., Xu, H., Xu, Q., Chen, B., and Kan, H.: Fine particulate matter constituents and cardiopulmonary mortality in a heavily polluted Chinese city, Environ. Health Persp., 120, 373–378, 2012.

Eck, T. F., Holben, B. N., Reid, J. S., Dubovik, O., Smirnov, A., O'Neill, N. T., Slutsker, I., and Kinne, S.: Wavelength dependence of the optical depth of biomass burning, urban, and desert dust aerosols, J. Geophys. Res.-Atmos., 104, 31333–31349, doi:10.1029/1999jd900923, 1999.

Green, M., Kondragunta, S., Ciren, P., and Xu, C.: Comparison of GOES and MODIS aerosol optical depth (AOD) to aerosol robotic network (AERONET) AOD and IMPROVE $PM_{2.5}$ mass at Bondville, Illinois, JAPCA J. Air Waste Ma., 59, 1082–1091, 2009.

Holben, B., Eck, T., Slutsker, I., Tanre, D., Buis, J., Setzer, A., Vermote, E., Reagan, J., Kaufman, Y., and Nakajima, T.: AERONET – a federated instrument network and data archive for aerosol characterization, Remote Sens. Environ., 66, 1–16, 1998.

Hsu, N. C., Jeong, M. J., Bettenhausen, C., Sayer, A. M., Hansell, R., Seftor, C. S., Huang, J., and Tsay, S. C.: Enhanced Deep Blue aerosol retrieval algorithm: the second generation, J. Geophys. Res.-Atmos., 118, 9296–9315, doi:10.1002/jgrd.50712, 2013.

Jackson, J. M., Liu, H., Laszlo, I., Kondragunta, S., Remer, L. A., Huang, J., and Huang, H. C.: Suomi-NPP VIIRS aerosol algorithms and data products, J. Geophys. Res.-Atmos., 118, 12673–12689, 2013.

Lee, J., Kim, J., Song, C. H., Ryu, J.-H., Ahn, Y.-H., and Song, C.: Algorithm for retrieval of aerosol optical properties over the ocean from the Geostationary Ocean Color Imager, Remote Sens. Environ., 114, 1077–1088, 2010.

Lee, J., Kim, J., Yang, P., and Hsu, N. C.: Improvement of aerosol optical depth retrieval from MODIS spectral reflectance over the global ocean using new aerosol models archived from AERONET inversion data and tri-axial ellipsoidal dust database, Atmos. Chem. Phys., 12, 7087–7102, doi:10.5194/acp-12-7087-2012, 2012.

Levy, R. C., Mattoo, S., Munchak, L. A., Remer, L. A., Sayer, A. M., Patadia, F., and Hsu, N. C.: The Collection 6 MODIS aerosol products over land and ocean, Atmos. Meas. Tech., 6, 2989–3034, doi:10.5194/amt-6-2989-2013, 2013.






ACPD
15, 20709–20741, 2015

Liu, H., Remer, L. A., Huang, J., Huang, H. C., Kondragunta, S., Laszlo, I., Oo, M., and Jackson, J. M.: Preliminary evaluation of S-NPP VIIRS aerosol optical thickness, J. Geophys. Res.-Atmos., 119, 3942–3962, 2014.

Munchak, L. A., Levy, R. C., Mattoo, S., Remer, L. A., Holben, B. N., Schafer, J. S., Hostetler, C. A., and Ferrare, R. A.: MODIS 3 km aerosol product: applications over land in an urban/suburban region, Atmos. Meas. Tech., 6, 1747–1759, doi:10.5194/amt-6-1747-2013, 2013.

Ohara, T., Akimoto, H., Kurokawa, J., Horii, N., Yamaji, K., Yan, X., and Hayasaka, T.: An Asian emission inventory of anthropogenic emission sources for the period 1980–2020, Atmos. Chem. Phys., 7, 4419–4444, doi:10.5194/acp-7-4419-2007, 2007.

Park, M. E., Song, C. H., Park, R. S., Lee, J., Kim, J., Lee, S., Woo, J.-H., Carmichael, G. R., Eck, T. F., Holben, B. N., Lee, S.-S., Song, C. K., and Hong, Y. D.: New approach to monitor transboundary particulate pollution over Northeast Asia, Atmos. Chem. Phys., 14, 659–674, doi:10.5194/acp-14-659-2014, 2014.

Petrenko, M., Ichoku, C., and Leptoukh, G.: Multi-sensor Aerosol Products Sampling System (MAPSS), Atmos. Meas. Tech., 5, 913–926, doi:10.5194/amt-5-913-2012, 2012.

Pope III, C. A., Ezzati, M., and Dockery, D. W.: Fine-particulate air pollution and life expectancy in the United States, New Engl. J. Med., 360, 376–386, 2009.

Remer, L. A., Kaufman, Y., Tanré, D., Mattoo, S., Chu, D., Martins, J. V., Li, R.-R., Ichoku, C., Levy, R., and Kleidman, R.: The MODIS aerosol algorithm, products, and validation, J. Atmos. Sci., 62, 947–973, 2005.

Remer, L. A., Mattoo, S., Levy, R. C., and Munchak, L. A.: MODIS 3 km aerosol product: algorithm and global perspective, Atmos. Meas. Tech., 6, 1829–1844, doi:10.5194/amt-6-1829-2013, 2013.

Sano, I., Mukai, S., Holben, B., Nakata, M., Yonemitsu, M., Sugimoto, N., Fujito, T., Hiraki, T., Iguchi, N., and Kozai, K.: DRAGON-West Japan campaign in 2012: regional aerosol measurements over Osaka, in: Proc. SPIE 8523, Remote Sensing of the Atmosphere, Clouds, and Precipitation IV, 85231 M, 2012.

Smirnov, A., Holben, B. N., Eck, T. F., Dubovik, O., and Slutsker, I.: Cloud-screening and quality control algorithms for the AERONET database, Remote Sens. Environ., 73, 337–349, doi:10.1016/S0034-4257(00)00109-7, 2000.

Vermote, E., Justice, C., and Csiszar, I.: Early evaluation of the VIIRS calibration, cloud mask and surface reflectance Earth data records, Remote Sens. Environ., 148, 134–145, 2014.





ACPD

15, 20709–20741, 2015



Title Page

Abstract | Introduction

Conclusions | References

Tables | Figures

◂ | ▸

Back | Close

Full Screen / Esc

Printer-friendly Version

Interactive Discussion

**Table 1.** Characteristics and quality control criteria of satellite aerosol products.

| Dataset | Including Criteria | Resolution | Coverage |
|---|---|---|---|
| VIIRS EDR | Quality Flag = High | 6 km, daily | Global |
| VIIRS IP | Quality Flag = High | 0.75 km, daily | Global |
| GOCI | Quality Flag = 3 | 6 km, 8 hourly obs. per day | East Asia |
| Auqa MODIS C6 3 km | Quality Flag = 3 | 3 km, daily | Global |
| Terra MODIS C6 3 km | Quality Flag = 3 | 3 km, daily | Global |





ACPD
15, 20709–20741, 2015

**Table 2.** Characteristics of ground AOD measurement datasets.

| | | Temporal Comparison | Spatial Comparison |
|---|---|---|---|
| Beijing | Data Set | AERONET | Microtops II |
| | Including Criteria | Level 1.5 | Median/SD < 2 |
| | Study Period | Jul 2012–Jun 2013 | Jan 2012–Jun 2013 |
| East Asia | Data Set | AERONET | DRAGON |
| | Including Criteria | Level 2.0 | Level 2.0 |
| | Study Period | Jul 2012–Jun 2013 | 15 Feb–31 May |





ACPD
15, 20709–20741, 2015

**Table 3.** Statistics of the temporal and spatial comparisons between satellite retrievals and ground AOD measurements at 550 nm in Beijing.

| | *N* | $R^2$ | Slope | Intercept | Bias | %EE |
|---|---|---|---|---|---|---|
| Temporal Comparison | | | | | | |
| VIIRS EDR | 90 | 0.70 | 0.96 | 0.12 | 0.11 | 52 |
| VIIRS IP | 133 | 0.63 | 1.00 | 0.25 | 0.25 | 32 |
| GOCI | 142 | 0.88 | 0.95 | 0.05 | 0.02 | 55 |
| GOCI all obs. | 957 | 0.88 | 0.98 | 0.008 | −0.006 | 59 |
| Aqua MODIS C6 3 km | 119 | 0.81 | 1.05 | 0.19 | 0.21 | 44 |
| Terra MODIS C6 3 km | 133 | 0.8 | 0.99 | 0.30 | 0.29 | 25 |
| Spatial Comparison | | | | | | |
| VIIRS EDR | 108 | 0.14 | 0.25 | 0.34 | 0.04 | 51 |
| VIIRS IP | 150 | 0.16 | 0.34 | 0.45 | 0.18 | 33 |
| GOCI | 208 | 0.44 | 0.75 | 0.07 | −0.11 | 31 |
| Aqua MODIS C6 3 km | 77 | 0.68 | 1.19 | 0.22 | 0.31 | 16 |
| Terra MODIS C6 3 km | 73 | 0.85 | 1.00 | 0.30 | 0.30 | 26 |

**Table 4.** Statistics of the temporal and spatial comparisons between satellite retrievals and ground AOD measurements at 550 nm over East Asia.

| | *N* | $R^2$ | Slope | Intercept | Bias | %EE |
|---|---|---|---|---|---|---|
| Temporal Comparison | | | | | | |
| VIIRS EDR | 601 | 0.74 | 0.96 | 0.06 | 0.05 | 64 |
| VIIRS IP | 437 | 0.55 | 1.03 | 0.14 | 0.15 | 37 |
| GOCI | 343 | 0.80 | 1.04 | 0.02 | 0.04 | 62 |
| GOCI all obs. | 2774 | 0.82 | 1.03 | 0.00 | 0.01 | 66 |
| Aqua MODIS C6 3 km | 180 | 0.71 | 1.00 | 0.08 | 0.08 | 56 |
| Terra MODIS C6 3 km | 197 | 0.70 | 1.06 | 0.14 | 0.16 | 39 |
| Spatial Comparison | | | | | | |
| VIIRS EDR | 144 | 0.53 | 0.96 | 0.18 | 0.16 | 41 |
| VIIRS IP | 229 | 0.60 | 1.11 | 0.21 | 0.26 | 26 |
| GOCI | 196 | 0.79 | 1.19 | −0.09 | 0.03 | 48 |
| Aqua MODIS C6 3 km | 108 | 0.81 | 1.26 | 0.07 | 0.19 | 28 |
| Terra MODIS C6 3 km | 132 | 0.73 | 1.00 | 0.23 | 0.23 | 27 |

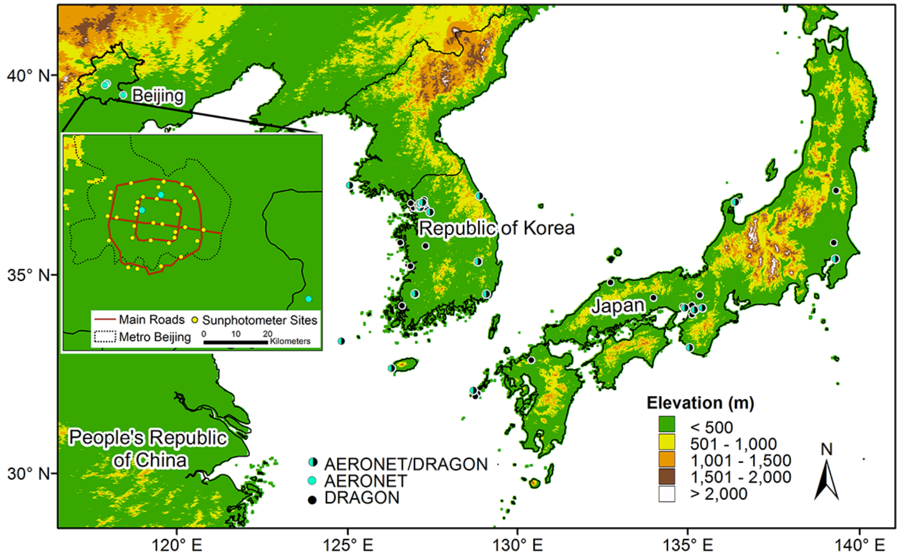


**Figure 1.** Study area showing all the ground AOD measurement sites.





ACPD
15, 20709–20741, 2015

Evaluation of VIIRS, GOCI, and MODIS Collection 6 AOD retrievals

Q. Xiao et al.

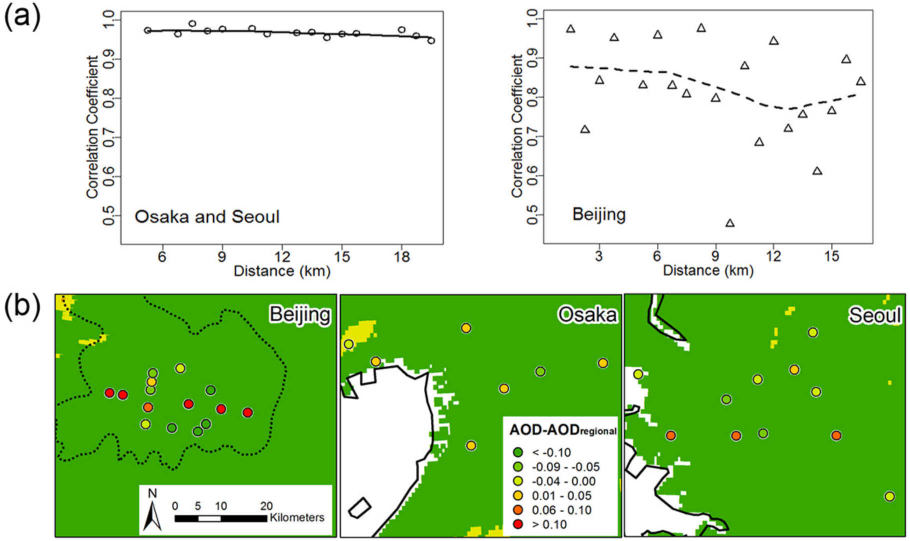


**Figure 2. (a)** The station to station correlation coefficients of daily mean AOD stratified by distance over (left) DRAGON-Asia region (right) Beijing region. The line is the Loess curvy. **(b)** The spatial distribution of average AOD in these three cities.



ACPD
15, 20709–20741, 2015

Evaluation of VIIRS, GOCI, and MODIS Collection 6 AOD retrievals

Q. Xiao et al.

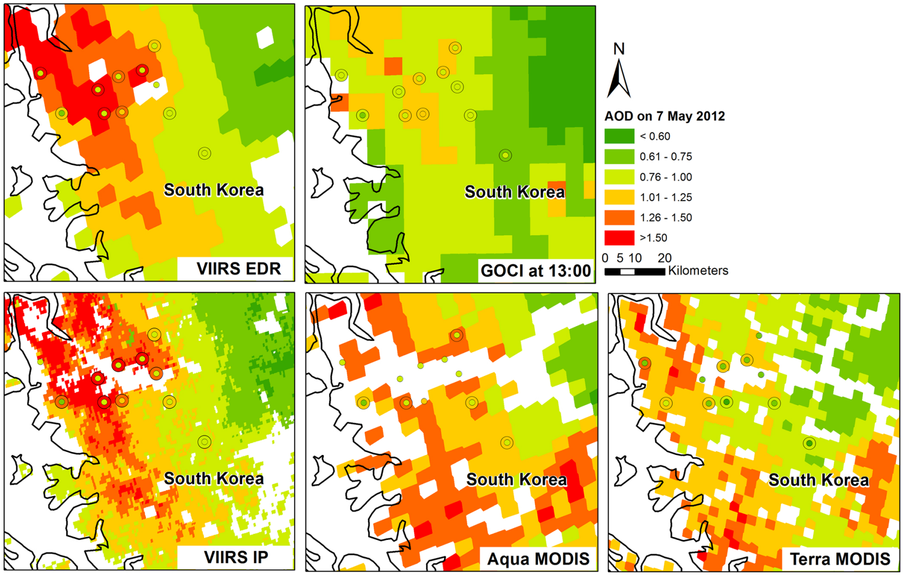


**Figure 3.** The AOD retrievals at 550 nm from different satellite aerosol products at their designed resolution on 7 May 2012. Retrieval/DRAGON collections are shown in double circles: the inner circle is the average DRAGON observations within ±30 min of satellite overpass and the outer circle is the satellite retrievals that the DRAGON stations falls in.



ACPD
15, 20709–20741, 2015

Evaluation of VIIRS, GOCI, and MODIS Collection 6 AOD retrievals

Q. Xiao et al.

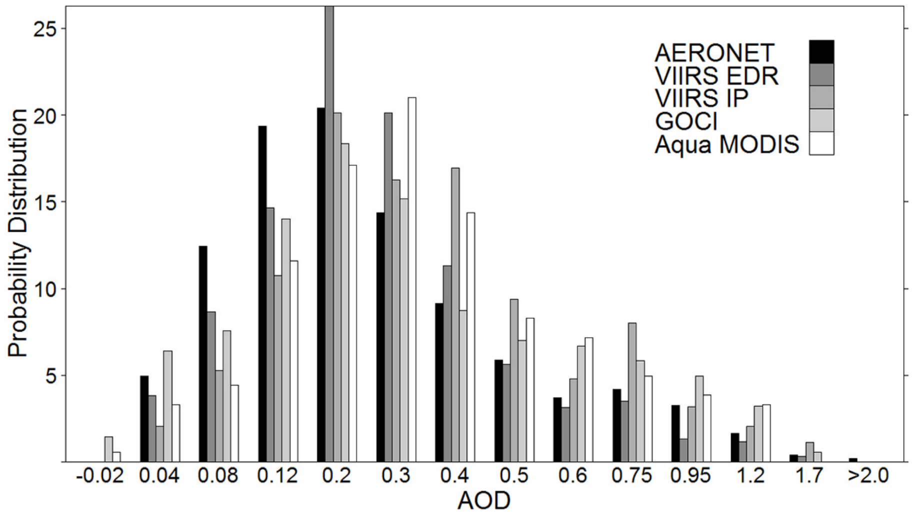


**Figure 4.** Histogram for the matched satellite AOD retrievals and AERONET measurements.



ACPD
15, 20709–20741, 2015

Evaluation of VIIRS, GOCI, and MODIS Collection 6 AOD retrievals

Q. Xiao et al.

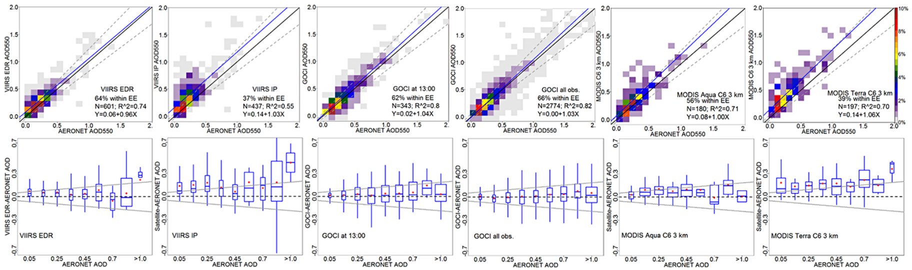


**Figure 5.** Upper – frequency scatter plots of satellite AOD retrievals against AERONET AOD measurements at 550 nm over Japan–South Korea region. The linear regression is shown as solid blue line, the boundary lines of the expected error are shown in the dash lines, and the one-one line is shown as solid black lines for reference. Lower – box plots of AOD errors (satellite – AERONET) vs. AERONET AOD over Japan–South Korea region. The one-one line (zero error) is shown in dash line and the boundary lines of the expected error are shown in gray solid lines. For each box-whisker, its properties and representing statistics include: width is $\sigma$ of the satellite AOD; height is the interquartile range of AOD error; whisker is the $2\sigma$ of the AOD error; middle line is the median of the AOD error; and red dot is the mean of the AOD error.





ACPD
15, 20709–20741, 2015

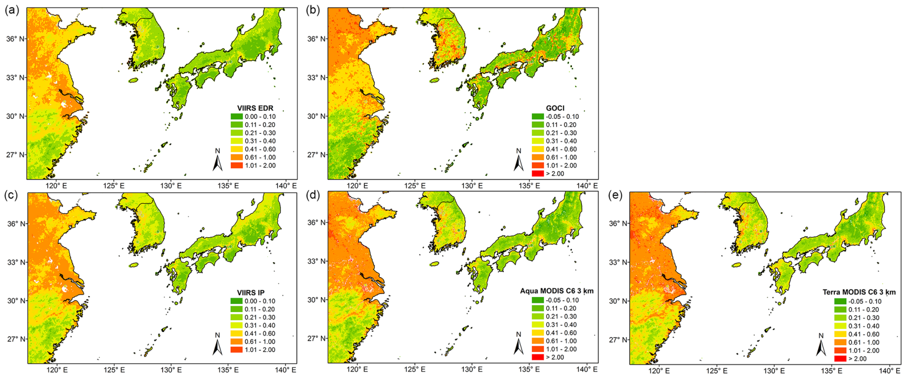


**Figure 6.** The distributions of the twelve months average AOD values from July 2012 to June 2013 from **(a)** VIIRS EDR, **(b)** GOCI, **(c)** VIIRS IP, **(d)** Aqua MODIS C6 3 km, and **(e)** Terra MODIS C6 3 km datasets.





ACPD
15, 20709–20741, 2015

Evaluation of VIIRS, GOCI, and MODIS Collection 6 AOD retrievals

Q. Xiao et al.

Title Page
Abstract | Introduction
Conclusions | References
Tables | Figures
◀I | ▶I
◀ | ▶
Back | Close
Full Screen / Esc
Printer-friendly Version
Interactive Discussion